Coexistence of Antiferromagnetism with Superconductivity in $CePt_2In_7$: Microscopic Phase Diagram Determined by ^{115}In NMR and NQR

H. Sakai,[1*] Y. Tokunaga,[1] S. Kambe,[1] F. Ronning,[2] E. D. Bauer,[2] and J. D. Thompson[2]
[1]Advanced Science Research Center, Japan Atomic Energy Agency, Tokai, Ibaraki 319-1195, Japan
[2]Los Alamos National Laboratory, Los Alamos, New Mexico 87545, USA
(Received 9 December 2013; revised manuscript received 9 March 2014; published 20 May 2014)

Single crystals of the heavy-fermion antiferromagnet $CePt_2In_7$ with a Néel temperature (T_N) of 5.2 K at ambient pressure have been investigated by zero-field ^{115}In-nuclear magnetic and quadrupole resonance measurements as a function of applied pressure. Within the antiferromagnetic state, the character of Ce's $4f$ electron appears to change from localized to itinerantlike at $P^* \sim 2.4$ GPa, approximately the pressure where superconductivity first emerges. With increased pressure, the superconducting transition T_c reaches a maximum just at or slightly before antiferromagnetic order disappears, and not at the pressure $P_c \sim 3.4$ GPa, where the steeply decreasing Néel boundary extrapolates to zero temperature. For $P > P_c$, the spin relaxation rate drops sharply by more than 2 orders of magnitude at T_c, suggestive of a first-order transition.

DOI: 10.1103/PhysRevLett.112.206401 PACS numbers: 71.27.+a, 73.43.Nq, 74.70.Tx, 76.60.-k

Quantum phase transitions in d- and f-electron materials, in which a second-order magnetic transition is suppressed to absolute zero temperature, continue to be the subject of intense research [1]. Currently, debate focuses on the applicability of two leading scenarios to explain the non-Fermi-liquid (NFL) behavior of the physical properties and the unconventional superconductivity that arises near the quantum critical point (QCP) in heavy fermion compounds. In the first, Hertz-Millis-Moriya (HMM) scenario [2–4], the Kondo temperature T_K remains finite at the QCP, and scattering of the itinerant conduction electrons by quantum fluctuations of a spin-density instability of a large Fermi surface lead to NFL behaviors [1]. At such a QCP, quantum critical fluctuations induce an attractive pair interaction for unconventional superconductivity, which appears to be realized in $CeCu_2Si_2$, $CePd_2Si_2$, and $CeIn_3$ [5].

If the Kondo scale vanishes at the QCP, new critical modes associated with destruction of the Kondo effect, in addition to fluctuations of an antiferromagnetic order parameter, control physical properties. A growing number of heavy fermion materials appear to exhibit behavior consistent with this second, Kondo breakdown or local quantum criticality scenario [6,7]. Upon crossing this QCP, a small Fermi surface characteristic of the magnetic state jumps sharply to a large Fermi surface in the paramagnetic (PM) state—in contrast to the HMM model in which the Fermi surface evolves continuously through the QCP [1]. This local quantum criticality model accounts for the behavior of $CeCu_{6-x}Au_x$ ($x = 0.1$) [8] and $YbRh_2Si_2$ [9]. $CeRhIn_5$ also appears to be close to a local QCP, where a discontinuous change from a small to a large Fermi surface coincides with its pressure-tuned $T = 0$ magnetic-nonmagnetic boundary [10,11]. In addition, it has been suggested that local fluctuations may also mediate the unconventional superconductivity near P_c with $T_c^{\max} = 2.6$ K [11,12].

To make progress towards understanding quantum phase transitions, new examples of quantum critical materials are necessary to test the applicability of the relevant theoretical models and to guide in the development of new ones. In this Letter, we report ^{115}In-nuclear magnetic and quadrupole resonance (NMR and NQR, respectively) measurements on the bilayer variant in the $Ce_mM_nIn_{3m+2n}$ family, $CePt_2In_7$ (with $m = 1$ $CeIn_3$ and $n = 2$ $PtIn_2$ layers), using a clean tuning parameter, pressure, to probe the quantum critical behavior around $P_c = 3.4$ GPa, where NFL behavior has been found [13]. The NQR and NMR measurements reveal two, well separated, characteristic pressures P^* and P_c in a T-P phase diagram: a localized-itinerant transition of the Ce $4f$ electron occurs at $P^* = 2.4$ GPa, while the antiferromagnetic (AFM) state disappears around $P_c = 3.4$ GPa. Between P^* and P_c, the AFM state is driven by itinerant $4f$ electrons and coexists with pressure-induced superconductivity. In the related material $CeRhIn_5$ ($n = 1$, $m = 1$), $P^* \simeq P_c$ [10,11,14]. $CePt_2In_7$ demonstrates, however, that P^* and P_c are not necessarily coincident.

Single crystals of $CePt_2In_7$ were grown by the self-flux method [15]. Hydrostatic pressures up to 3.7 GPa were applied with a standard hybrid-cylinder cell and an indenter-type cell [16] using Daphne7373 oil as a pressure medium. Pressures were determined by ^{63}Cu-NQR frequencies in Cu_2O [17]. As shown in Fig. 1(a), there are three crystallographically inequivalent In sites, denoted as In(1) for $2b$ in Wyckoff notation, In(2) for $4d$, and In(3) for $8g$ sites, respectively. As reported previously [18], all NQR lines are successfully assigned. In order to investigate

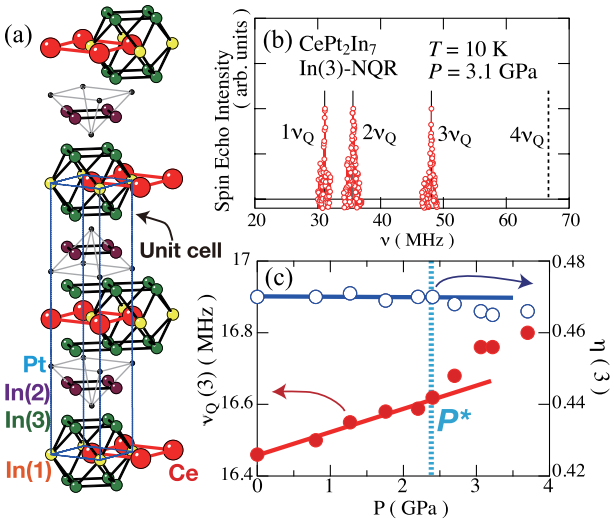

FIG. 1 (color online). (a) Crystal structure of $CePt_2In_7$. (b) NQR spectrum for In(3) sites in $CePt_2In_7$ under 3.1 GPa at 10 K. The dashed line indicates a calculated resonance position of $4\nu_Q$. (c) Pressure dependence of ν_Q and η for In(3) in $CePt_2In_7$.

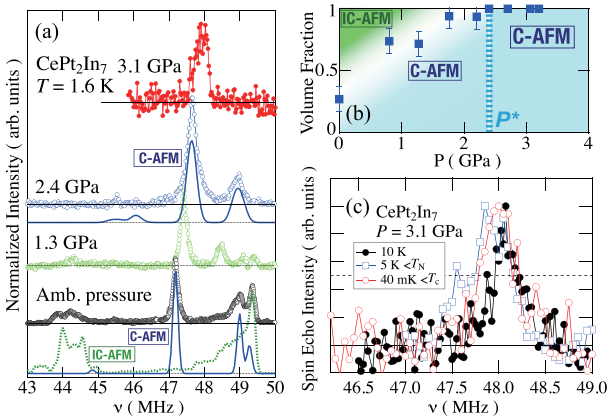

FIG. 2 (color online). (a) Pressure variation at 1.6 K of the NMR spectrum for $3\nu_Q$ of In(3) sites. The simulated curves at ambient pressure and 2.4 GPa are also plotted [18]. (b) Pressure dependence of the estimated volume fraction of the C-AFM portion [18]. (c) NQR and NMR spectra of $3\nu_Q$ line for In(3) sites under 3.1 GPa at several temperatures of 40 mK, 5 K, and 10 K.

the relation between magnetism and superconductivity, we chose the In(3) sites, because the internal field in the AFM state is not canceled on these sites. On the other hand, the In(1) sites in $CePt_2In_7$ are closely analogous to the In sites in the relative $CeIn_3$ or the In(1) sites in $CeRhIn_5$, on which the internal field is canceled completely in $CePt_2In_7$ [18] or partially in $CeIn_3$ [19] and $CeRhIn_5$ [20].

First, we present evidence for a transition from localized to itinerant behavior of the Ce $4f$ electron in $CePt_2In_7$. The NQR spectrum of the orthorhombic In(3) sites at 10 K and 3.1 GPa is shown in Fig. 1(b). From the line positions, the nuclear quadrupole frequency $\nu_Q = 16.76$ MHz and asymmetry parameter $\eta = 0.466$ are determined, where $\nu_Q = 3e^2qQ/\{2I(2I-1)h\}$, eQ is the nuclear quadrupolar moment, and the principal component of the local electric field gradient (EFG) tensor $eq \equiv V_{ZZ}$ is given by $\eta \equiv |V_{XX} - V_{YY}|/V_{ZZ}$. The electric quadrupole Hamiltonian matrix was numerically diagonalized to fit the resonant positions obtained at each pressure, yielding the pressure dependence of ν_Q and η displayed in Fig. 1(c). The quadrupole frequency ν_Q increases linearly with increasing pressure up to ~2 GPa, but an abrupt kink in ν_Q is observed at $P^* \sim 2.4$ GPa, where a similar kink is also seen in η. The EFG is a good parameter to evaluate the degree of $4f$ delocalization in the CeMIn$_5$ series. [21] Therefore, we interpret this kink as signaling a change in the charge distribution from surrounding ions and electrons, that is the consequence of a Ce $4f$ electron localized-to-itinerant transition resulting from a pressure-induced increase in c-f hybridization. Such a deviation of the ν_Q-P trend in the prototypical material $CeCu_2Si_2$ is seen as well, reflecting a crossover of the $4f$ nature [22].

A change in the internal magnetic field associated with the AFM order also provides evidence for a localized-to-itinerant transition of the Ce $4f$ electron in $CePt_2In_7$. As reported previously [18,23], the NQR spectra at ambient pressure is explained by the coexistence of an incommensurate (IC-) and commensurate (C-) AFM component of the magnetic structure. As shown in Figs. 2(a) and 2(b), the volume fraction of the IC-AFM component, deduced from the $3\nu_Q$ spectra at the In(3) sites, gradually decreases with applied pressure and is completely suppressed above ~2.4 GPa, where only the C-AFM component persists. The pressure dependence of the estimated internal field $H_{\rm int}$ on In(3) sites is summarized in Fig. 4(b) to illustrate its relationship to the T-P phase diagram. A large decrease of the internal field occurs around $P^* \sim 2.4$ GPa and is consistent with a change of localized-to-itinerant f character in the AFM state, as observed experimentally [10] and predicted theoretically [24] in $CeRhIn_5$. At 3.1 GPa [Fig. 2(c)], a change in the line width provides an estimate of the internal field of about 150 Oe on the In(3) sites, corresponding to no more than ~3% of the amplitude at ambient pressure. These observations of the EFG and $H_{\rm int}$ suggest that the AFM state is driven by itinerant $4f$ electrons above P^*. Assuming the hyperfine coupling constant is pressure independent, this reduction of the internal field above 2.4 GPa corresponds to a drastic reduction in the ordered moment and is typical of a spin-density wave (SDW). No significant broadening is observed below the superconducting (SC) transition temperature $T_c = 2$ K; i.e., the onset of SC does not substantially disturb the AFM state. We note that the spectrum at 3.7 GPa, where the AFM state disappears completely, does not show such an additional broadening from the NQR line width as temperature decreases.

Measurements of the spin-lattice relaxation rate $1/T_1$ further characterize the evolution of the normal state and the coexistence of superconductivity and magnetism with applied pressure. The nuclear magnetization recovery from a saturation ($\pi/2$) or an inversion (π) rf pulse was measured as a function of time at the $3\nu_Q$ line of the In(3) sites for a given temperature and pressure. T_1 was derived from fitting to the appropriate relaxation function [25] calculated by using η experimentally determined at each pressure [Fig. 1(c)]. In the coexisting region of AFM and SC states, the fitting was made after ~50% of nuclear magnetization was recovered in order to pick the longer T_1 associated with SC.

At ambient pressure, the spin-lattice relaxation rate divided by temperature $(T_1T)^{-1}$ follows a Curie-Weiss-like behavior above $T^* \sim 30$ K, indicating fully localized Ce $4f$ moments [18]. At temperatures below 30 K and pressures up to 2.4 GPa, $(T_1T)^{-1}$ shows a weaker temperature dependence down to 10 K and is nearly pressure independent, as displayed in Fig. 3(b), although the values of $(T_1T)^{-1}$ are gradually suppressed by pressure. A gradual increase of $(T_1T)^{-1}$ as the temperature decreases below ~10 K indicates an enhancement of AFM spin fluctuations. Upon further cooling, $(T_1T)^{-1}$ exhibits a sharp peak at $T_N(P)$ reflecting the critical slowing down and an AFM gap opening just below $T_N(P)$. Thus, the pressure dependence of T_N can be tracked by the sharp peak of $(T_1T)^{-1}$, as plotted in Fig. 4(a), while kink anomalies of resistivity and ac calorimetry at $T_N(P)$ are rounded [13]. Near the occurrence of superconductivity at 2.7 GPa, denoted by the arrow in Fig. 3(c), $(T_1T)^{-1}$ gradually increases below 0.3 K, implying a temperature evolution of the spin fluctuations within the C-AFM state. This slope of $(T_1T)^{-1}$ below 0.3 K appears to be nearly pressure independent between 2.7 and 3.7 GPa; therefore, this behavior does not reflect SC fluctuations nor spin fluctuations by uncompensated localized Ce moments, as found in lightly La-substituted $Ce_{0.97}La_{0.03}RhIn_5$ [26]. A more likely scenario is that these fluctuations are due to a Fermi surface instability at $P^* = 2.4$ GPa reflected in the change in ν_Q and $H_{\rm int}$ [Figs. 1(c) and 2(c)].

As shown in Fig. 3(a), $1/T_1$ peaks sharply at $T_N(P) =$ 5.2 K and then follows a Korringa-like behavior, i.e., $1/T_1 \propto T$, below $T_N(P)$. An additional decrease at $T_c(P)$ with no coherence peak suggests that non-s-wave, bulk SC emerges from the AFM phase. The Korringa law above the $T_c(P)$ indicates the presence of heavy

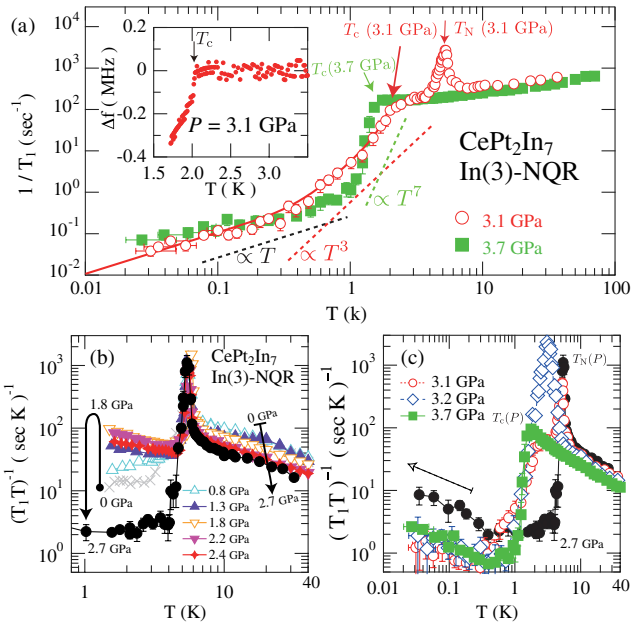

FIG. 3 (color online). (a) Temperature dependence of nuclear spin-lattice relaxation rates $1/T_1$ for In(3) sites in $CePt_2In_7$ under the pressures of 3.1 and 3.7 GPa. The solid curve represents a tentative fit by a simple d wave model. The dotted lines are guides to the eye. The inset shows the temperature dependence of resonant frequency shifts of an *in situ* rf circuit at $P = 3.1$ GPa. Temperature dependence of $(T_1T)^{-1}$ under several pressures of (b) 0, 0.8, 1.3, 1.8, 2.2, 2.4, and 2.7 GPa and (c) 2.7, 3.1, 3.2, and 3.7 GPa.

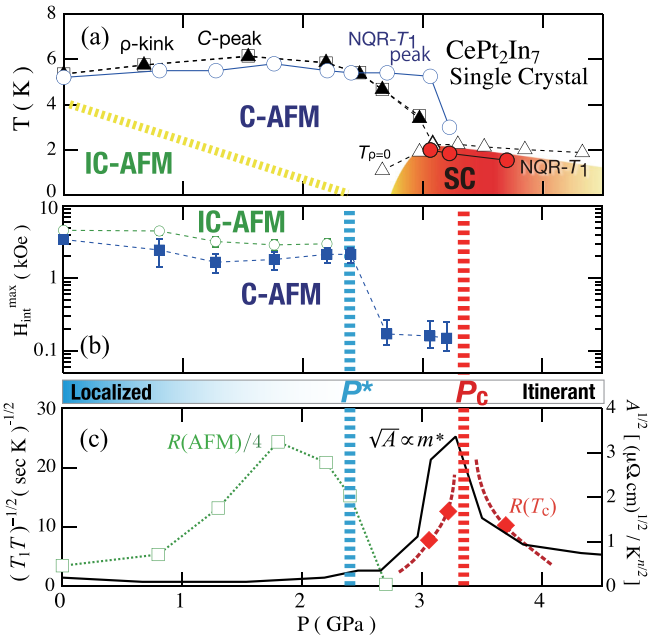

FIG. 4 (color online). (a) T-P phase diagram for single crystals of $CePt_2In_7$. The results from resistivity and ac-calorimetry measurements [13] are also plotted. The bold dotted line is schematically drawn as a boundary between C-AFM and IC-AFM, which is a first-order transition. (b) Pressure dependence of the maximum internal field on the In(3) sites. The longitudinal axis is logarithmic. The bottom bar schematically indicates the $4f$ character. (c) Pressure dependence of $(T_1T)^{-1/2}$ just above $T_c(P)$, above and below $T_N(P)$. The dotted curve is a guide to the eye, describing an enhancement of effective mass m^*. The square root of the A coefficient from the resistivity at low temperatures [13] is also plotted as a measure of m^*.

quasiparticles that are not gapped by the AFM ordering. Bulk superconductivity is also confirmed by *in situ* ac-susceptibility measurements where a clear frequency shift is observed at $T_c(3.1\ \mathrm{GPa}) = 2$ K, as shown in the inset in Fig. 3(a). The T dependence of $1/T_1$ below $T_c(P)$ obeys a T^3 law over 3 orders of magnitude, suggesting the existence of line nodes in the SC gap. The $1/T_1$ data deviate from T^3 behavior well below $T_c(P)$ and show a Korringa law again. At 3.1 GPa, where superconductivity and C-AFM coexist, a fit of a polar type $\Delta = \Delta_0(T)\cos\theta$ gap function to the $1/T_1$ data, assuming a simple spherical Fermi surface, yields a gap value of $2\Delta_0(0) \sim 13 k_B T_c$. This analysis indicates strong coupling line-nodal superconductivity and a ratio of residual density of states (DOS) to the value at $T_c(P)$ of 0.15. This gap value is larger than found in $CeRhIn_5$ by NQR measurements, where $2\Delta_0(0) \sim 6.6 k_B T_c$ [27]. At 3.7 GPa, the C-AFM ordering is completely suppressed, and $1/T_1$ decreases very rapidly just below T_c, as shown in Fig. 3(a), with $1/T_1 \propto T^7$. Specific heat measurements of $CePt_2In_7$ [13] reveal that the jump at $T_c(P)$ is only about 5 times larger in the region where superconductivity is observed compared to the small jump in the AFM + SC coexistence region. This increase in the SC gap is not large enough to explain the sharp decrease in $1/T_1$; indeed, a simple d-wave fit leads to an unphysical magnitude of the SC gap $2\Delta_0(0) \sim 70 k_B T_c$ and cannot be explained by a point-node gap or an extended d-wave gap with higher harmonics [28]. An alternative explanation—not captured within either HMM or local QCP scenarios—involves coupling of the SC order parameter to another, undetermined order, resulting in a first-order transition, which presumably occurs above the QCP at $P_c = 3.4$ GPa.

At the intermediate pressure of 3.2 GPa, the Néel temperature T_N decreases from ~5 to 3 K. As seen in Fig. 4(a), the slope of T_N is very steep, of the order of $dT_N/dP \sim -10$ K/GPa (even if taking the pressure distribution of $|\Delta P| < 0.1$ GPa at most) with a critical pressure for C-AFM at $P_c = 3.4$ GPa. Finally, at 3.7 GPa, as shown in Fig. 3(c), $(T_1T)^{-1}$ shows only a very rapid drop at the SC transition $T_c(3.7\ \mathrm{GPa}) = 1.5$ K.

The In(3) NQR measurements on $CePt_2In_7$ also reveal the evolution of the electronic and magnetic properties under pressure. The pressure-temperature phase diagram of $CePt_2In_7$ is displayed in Fig. 4(a). The C-AFM component is stabilized under pressure, with the suppression of the IC-AFM component occurring at $P^* \sim 2.4$ GPa. At this pressure, the $4f$ electrons in $CePt_2In_7$ become itinerant and bulk superconductivity emerges. A similar situation occurs in $CeRh_{1-x}Ir_xIn_5$ $(0.25 \le x \le 0.6)$, in which the development of bulk superconductivity coincides with the onset of a commensurate $[\boldsymbol{Q} = (1/2, 1/2, 1/2)]$ component of the AFM order, albeit which also coexists with an incommensurate component with a wave vector $\boldsymbol{Q} = (1/2, 1/2, 0.297)$ [29], characteristic of the parent $CeRhIn_5$ material [30].

The spin-lattice relaxation $(T_1T)^{-1}$ reflects the square of the DOS at the Fermi level with an electronic correlation factor. In Fig. 4(c), $(T_1T)^{-1/2}$ is plotted as a function of pressure. To avoid the critical slowing down just near $T_N(P)$, $R \equiv (T_1T)^{-1/2}$ for the PM state is estimated from the extrapolation to T_N from ~10 K and is nearly pressure independent; i.e., the small volume change by applied pressure up to ~4 GPa does not significantly affect the DOS and/or AFM correlations in the PM state. Below T_N, the values of $R(\mathrm{AFM})$ and $R(T_c)$ are determined at 1.5 K in the absence of a SC transition and at $T_c(P)$, respectively. As seen in Fig. 4(c), $R(\mathrm{AFM})$, i.e., the residual DOS and/or AFM correlations after opening the AFM gap at $T_N(P)$, changes substantially under applied pressure. $R(\mathrm{AFM})$ increases and reaches a maximum around 1.8 GPa where the IC-AFM component still coexists with C-AFM ordering at 1.5 K. Once the C-AFM component is fully stabilized above P^*, $R(\mathrm{AFM})$ decreases sharply. Near the QCP at $P_c = 3.4$ GPa, $R(\mathrm{AFM})$ or $R(T_c)$ increases, signaling a change in the effective mass at the lowest temperature. This conclusion is consistent with the P dependence of the A coefficient from low temperature resistivity with the form AT^n and $m^* \sim 160\ m_e$ near P_c determined by measurements of the upper critical field [13].

In summary, the pressure evolution of the AFM and SC states in $CePt_2In_7$ have been determined by NQR. In particular, the separate occurrence of a Ce $4f$ delocalization transition at P^* and magnetic QCP at P_c contrasts with the simultaneous occurrence of a $T = 0$ magnetic transition and a jump in Fermi volume where T_c is a maximum in $CeRhIn_5$ [10,11]. The reduced Kondo screening due to a more 2D lattice in $CePt_2In_7$ [31] might separate P^* from P_c. Equally unusual is a coupling of superconductivity to another order parameter suggested by the sharp, first-order-like drop in $1/T_1$ at 3.7 GPa [Fig. 3(a)]. It is interesting to note that, in both $CePt_2In_7$ and $CeRh_{0.5}Ir_{0.5}In_5$ [32], superconductivity reaches a maximum T_c inside the AFM state. One possibility is that the maximal T_c results from a competition for the Fermi surface involving the opening of the (large) C-SDW gap at P^* and the SC gap. Assuming the C-SDW gap deceases and the SC gap increases with applied pressure, T_c becomes maximal because of a tradeoff of available Fermi surface and the increased strength of quantum fluctuations of the SDW order, which are a maximum around the extrapolated QCP. None of these properties of $CePt_2In_7$ is obvious within the HMM scenario. The local criticality model predicts a jump from a small to large Fermi surface within the magnetic state [6,33]. In addition, a localized-to-itinerant transition has been theoretically predicted to occur *inside* AFM states in a general Kondo lattice [24]. So far, neither theoretical model can capture a difference of superconductivity across P^* and P_c, i.e., a first-order-like SC transition and its robustness against pressures. Recently, an enhancement of singlet superconductivity pairing at the local QCP has been

proposed [12], but additional coupling to AFM order must be developed to explain why $T_c^{\max}$ occurs within the AFM state in $CePt_2In_7$. By showing a clear separation of P^* and P_c, $CePt_2In_7$ is a particularly interesting system to investigate the relation of superconductivity near a QCP and a Fermi surface volume change, which may lead to a new or extended theoretical framework.

We thank S. Hoshino, N. Tateiwa, Y. Haga, and H. Yasuoka for valuable discussions. Work in Japan was supported by the Reimei Research Program of JAEA. Work at LANL was performed under the auspices of the U.S. DOE, Office of Basic Energy Sciences, Division of Materials Sciences and Engineering.

*sakai.hironori@jaea.go.jp

[1] H. v. Löhneysen, A. Rosch, M. Vojta, and P. Wölfle, Rev. Mod. Phys. **79**, 1015 (2007).
[2] J. A. Hertz, Phys. Rev. B **14**, 1165 (1976).
[3] A. J. Millis, Phys. Rev. B **48**, 7183 (1993).
[4] T. Moriya and T. Takimoto, J. Phys. Soc. Jpn. **64**, 960 (1995).
[5] P. Monthoux, D. Pines, and G. G. Lonzarich, Nature (London) **450**, 1177 (2007).
[6] Q. Si, S. Rabello, K. Ingersent, and J. L. Smith, Nature (London) **413**, 804 (2001).
[7] C. Pépin, Phys. Rev. B **77**, 245129 (2008).
[8] A. Schröder, G. Aeppli, E. Bucher, R. Ramazashvili, and P. Coleman, Phys. Rev. Lett. **80**, 5623 (1998).
[9] J. Custers, P. Gegenwart, H. Wilhelm, K. Neumaier, Y. Tokiwa, O. Trovarelli, C. Geibel, F. Steglich, C. Pépin, and P. Coleman, Nature (London) **424**, 524 (2003).
[10] H. Shishido, R. Settai, H. Harima, and Y. Ōnuki, J. Phys. Soc. Jpn. **74**, 1103 (2005).
[11] T. Park, F. Ronning, H. Q. Yuan, M. B. Salamon, R. Movshovich, J. L. Sarrao, and J. D. Thompson, Nature (London) **440**, 65 (2006).
[12] J. H. Pixley, L. Deng, K. Ingersent, and Q. Si, arXiv:1308.0839.
[13] V. A. Sidorov, X. Lu, T. Park, H. Lee, P. H. Tobash, R. E. Baumbach, F. Ronning, E. D. Bauer, and J. D. Thompson, Phys. Rev. B **88**, 020503(R) (2013).
[14] T. Park, V. A. Sidorov, F. Ronning, J. X. Zhu, Y. Tokiwa, H. Lee, E. D. Bauer, R. Movshovich, J. L. Sarrao, and J. D. Thompson, Nature (London) **456**, 366 (2008).
[15] P. H. Tobash, F. Ronning, J. D. Thompson, B. L. Scott, P. J. W. Moll, B. Batlogg, and E. D. Bauer, J. Phys. Condens. Matter **24**, 015601 (2012).
[16] T. C. Kobayashi, H. Hidaka, H. Kotegawa, K. Fujiwara, and M. I. Eremets, Rev. Sci. Instrum. **78**, 023909 (2007).
[17] K. Kitagawa, H. Gotou, T. Yagi, A. Yamada, T. Matsumoto, Y. Uwatoko, and M. Takigawa, J. Phys. Soc. Jpn. **79**, 024001 (2010).
[18] H. Sakai, Y. Tokunaga, S. Kambe, H. O. Lee, V. A. Sidorov, P. H. Tobash, F. Ronning, E. D. Bauer, and J. D. Thompson, Phys. Rev. B **83**, 140408(R) (2011).
[19] Y. Kohori, Y. Inoue, T. Kohara, G. Tomka, and P. C. Riedi, Physica (Amsterdam) **259–261B**, 103 (1999).
[20] N. J. Curro, P. C. Hammel, P. G. Pagliuso, J. L. Sarrao, J. D. Thompson, and Z. Fisk, Phys. Rev. B **62**, R6100 (2000).
[21] J. Rusz, P. M. Oppeneer, N. J. Curro, R. R. Urbano, B.-L. Young, S. Lebègue, P. G. Pagliuso, L. D. Pham, E. D. Bauer, J. L. Sarrao, and Z. Fisk, Phys. Rev. B **77**, 245124 (2008).
[22] T. C. Kobayashi, K. Fujiwara, K. Takeda, H. Harima, Y. Ikeda, T. Adachi, Y. Ohishi, C. Geibel, and F. Steglich, J. Phys. Soc. Jpn. **82**, 114701 (2013).
[23] H. Sakai, Y. Tokunaga, S. Kambe, H. Lee, V. A. Sidorov, P. H. Tobash, F. Ronning, E. D. Bauer, and J. D. Thompson, J. Phys. Conf. Ser. **391**, 012057 (2012).
[24] S. Hoshino and Y. Kuramoto, Phys. Rev. Lett. **111**, 026401 (2013).
[25] J. Chepin and J. J. H. Ross, J. Phys. Condens. Matter **3**, 8103 (1991).
[26] H. Sakai, N. Kurita, C. F. Miclea, R. Movshovich, H. O. Lee, F. Ronning, E. D. Bauer, and J. D. Thompson, J. Phys. Soc. Jpn. **80**, SA059 (2011).
[27] M. Yashima, H. Mukuda, Y. Kitaoka, H. Shishido, R. Settai, and Y. Ōnuki, Phys. Rev. B **79**, 214528 (2009).
[28] R. Prozorov, Supercond. Sci. Technol. **21**, 082003 (2008).
[29] A. Llobet, A. D. Christianson, W. Bao, J. S. Gardner, I. P. Swainson, J. W. Lynn, J. M. Mignot, K. Prokes, P. G. Pagliuso, N. O. Moreno, J. L. Sarrao, J. D. Thompson, and A. H. Lacerda, Phys. Rev. Lett. **95**, 217002 (2005).
[30] W. Bao, P. G. Pagliuso, J. L. Sarrao, J. D. Thompson, Z. Fisk, J. W. Lynn, and R. W. Erwin, Phys. Rev. B **62**, R14621 (2000).
[31] M. Matsumoto, M. J. Han, J. Otsuki, and S. Y. Savrasov, Phys. Rev. B **82**, 180515(R) (2010).
[32] P. G. Pagliuso, C. Petrovic, R. Movshovich, D. Hall, M. F. Hundley, J. L. Sarrao, J. D. Thompson, and Z. Fisk, Phys. Rev. B **64**, 100503(R) (2001).
[33] Q. Si, Phys. Status Solidi (b) **247**, 476 (2010).